

GEOELECTRICAL MODEL OF GEOTHERMAL SPRING IN IE JUE SEULAWAH DERIVING FROM 2D VLF-EM AND DC RESISTIVITY METHODS

Marwan^{1,2*}, Muhammad Isa², Rinaldi Idroes³, Nursyafira¹, Syafrizal Idris⁴, Muhammad Yanis¹, Azman Abdul Ghan⁵, Andri Yadi Paembonan⁶

¹Geophysical Engineering Department, Universitas Syiah Kuala, Darussalam–Banda Aceh 23111, Indonesia

²Physics Department, Universitas Syiah Kuala, Darussalam-Banda Aceh 23111, Indonesia

³Chemistry Department, Universitas Syiah Kuala, Darussalam-Banda Aceh 23111, Indonesia

⁴Physics Department, Universitas Malikussaleh, Lhokseumawe, 24351, Indonesia

⁵Department of Geology, University of Malaya, 50603 Kuala Lumpur, Federal Territory Malaysia

⁶Geophysical Engineering, Institut Teknologi Sumatera, Lampung 35365, Indonesia

* marwan.geo@unsyiah.ac.id

Seulawah Agam is one of the volcanic areas in Aceh province, Indonesia, which planned for a powerplant construction with an energy capacity expected to be approximately 230 MWe. This volcano has seven manifestations in the form of craters, hot water, and heated soil. The hydrothermal system in this volcano is controlled by a fault system which acts as a medium for the entry and exit of fluids. Therefore, understanding the local geology is required for geothermal power plant development, especially for the determination area for injection and production wells. In this research, we use the Very Low-Frequency Electromagnetic (VLF-EM) methods combined with electrical resistivity tomography data on the le Jue manifestation area to determine the shallow structure related to the manifestation. The VLF was made for 4 profiles with 700 m length for each VLF-EM profile and 300 m for electrical resistivity lines. We utilized the Karous Hjelt filter for qualitative interpretation, while Occam's algorithm was applied for 2D inversion of data for quantitative analysis of VLF-EM data. Based on the current density model, several vertical conductive anomalies can be well demonstrated at a distance of 300-400 m from the four VLF profiles. The conductive anomaly can also be seen in the resistivity data from the electrical resistivity. The results of the Occam model show that the depth of faults and fractures is seen at 30 m depth with low resistivity (below 100 Ω m). This anomaly is generally associated with outcrops in the field, such as fumarole and warm ground on the east side of the manifestation area. In addition, the 2D inversion model of VLF also shows the contrast of several fracture zones as a place for fluid to enter and exit the Seulawah volcano. Therefore, based on our result, it can be summed up that this method is effectively applied to geothermal in high terrain areas such as in Indonesia and can be used to suggest safe locations for injection wells and production of geothermal drilling.

Keywords: very low frequency, 2D inversion, hot spring, Seulawah Agam

1 INTRODUCTION

Indonesia is known for its territory, which is in the ring of the fire area. This cause it to have geothermal energy potential estimation to reach 40% of the total estimated geothermal energy in the world's volcanoes, which is approximate 28,617 MWe [1]. In the exploitation process, geothermal is one of the alternative sources known as green energy and only requires a small area for exploration and exploitation compared to conventional energy sources such as oil and gas. In the northernmost of Sumatra, Aceh Province has 20 potential geothermal fields that are potential to be developed by the government, such as the Jaboi volcano on Weh Island [2], Peut Sagoe [3], dan Seulawah Agam [4], [5] with an estimated electrical energy production capacity of 230 Mwe [6]. In addition, other parts of the geothermal site, geothermal sites have begun to be developed into geological-based tourist spots to directly impact the community's economy [7]. Various explorations method has been deployed in Seulawah to understand the geothermal system of the volcano, for example, geochemical studies [8] to determine water sources and predict subsurface temperatures, geophysical surveys conducted to study subsurface structures based on 2D and 3D resistivity models [6], where the results of the exploration study have shown that the reservoir layer as the primary target for geothermal exploration is at depths below 2 km [4]. Geographically the location of le Jue Seulawah Agam is shown in Fig.1.

Although various methods have been applied to study the geothermal system, these surveys are still regional, while local exploration focusing on specific manifestations is still minimally carried out to determine the shallow geological structure related to the manifestation. Local mechanisms influence the geology of the volcano in each manifestation, where it is known that Seulawah has seven different manifestations. Two are craters, and the other is hot water and warm ground [8]. One of which is the le Jue hot spring manifestation of le Jue in Aceh Besar. Although the volcano manifestation is found in 9 locations, the le Jue was chosen to study the shallow hydrothermal system of the volcano, which caused it to be easily accessible and far from an electrical infrastructure that interferes with VLF instruments. Meanwhile, Heutz and Cempaga craters are difficult to access at 1220 msl and close to the top of the volcano.

On the other hand, apart from the reservoir layer, fractures and faults are also a core part of exploration in geothermal energy studies because they have a role as reservoir flow paths for fluid production in the exploitation process [2], [9]. It is essential to study local tectonic settings in volcanic manifestation areas. Apart from studying the hydrothermal system, this information is also needed for determining the location of test and production wells in geothermal development, where an error in determining the location of the well can result in significant losses.

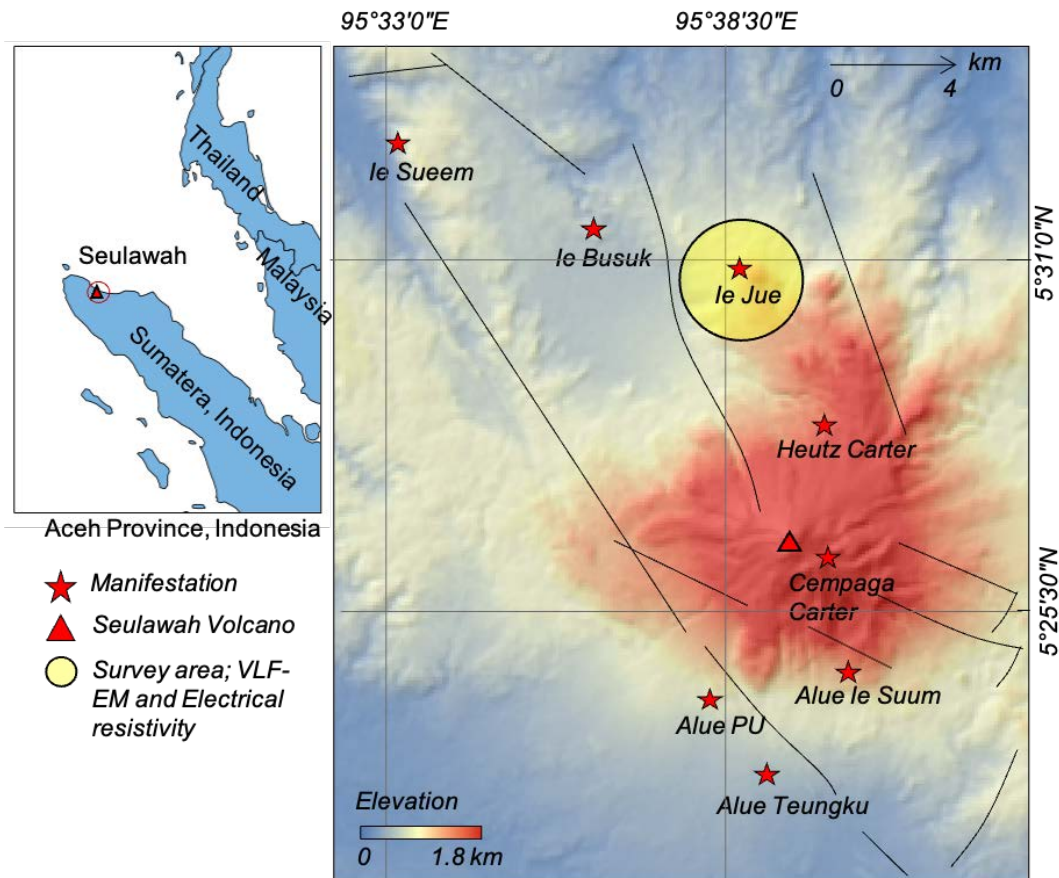


Fig.1. Distribution of Seulawah manifestations includes a crater and others, i.e., hot springs and warm ground around manifestation, the VLF-EM, and electrical resistivity only focused in the le Jue area, as shown in the yellow circle.

This study applies two near-surface geophysical methods, Very Low-Frequency Electromagnetic (VLF-EM), and electrical resistivity for hydrothermal mapping and fracture of the le Jue Seulawah Agam manifestation. Both methods have low costs and were effectively used for near-surface studies. They are also non-destructive field techniques. The VLF method is classified as passive electromagnetic because it uses a wave source that is emitted for military communication purposes with a frequency band range from 15-30 kHz to become an electromagnetic source for geophysical investigations. The VLF method has an economic advantage, and the operation is faster than another electromagnetic method in field operation. This method allows us to detect conductors below the surface [10].

The comprehensive method for shallow mapping structures is electrical resistivity [11]–[13], especially inaccessible areas where mobilization equipment is accessible. However, in areas that are difficult to access, such as Indonesian volcanoes located in high topography, it is necessary to develop an instrument that is easy to mobilize, such as VLF-EM. This method can be measured by only one person with a fast time than electrical resistivity [14]. The VLF method is also susceptible to conductors caused by hot water of the thermal spring flowing through fractures [2], [13], so the VLF applications need to be developed for shallow geothermal studies on several volcanoes. Therefore, we apply the VLF method and combine it with electrical resistivity as a commonly used method for shallow structures.

Thus, the VLF-EM method can be employed in the highly resistive area and high contact resistance where electrical resistivity surveys have limitations. Referring to the literature, the VLF application has been successfully implemented in several areas, such as Seferihisar geothermal in Western Anatolia [15], Hisar geothermal field in Demirci, western Turkey [13], and study the mud volcano in southern Taiwan [16]. On the other hand, the electrical resistivity method known as direct current (DC) resistivity is also used in this study to determine resistivity contrasts associated with water accumulation. The conventional electrical method is used to study variations in subsurface electrical resistivity parameters and is applied in assuming horizontally layered earth [17]. Both approaches have been widely used for shallow mapping anomalies less than 100 m below the surface [18]. By applying these two methods, we can reconstruct a more reliable model for interpretation. The advantage of the research is the use of the Occam algorithm for 2D inversion of VLF-EM data so that resistivity parameters are obtained that can be compared with the electrical resistivity method that has been measured in the same place.

2 GEOLOGY AND PREVIOUS RESEARCH

Indonesia is tier third in Southeast Asia in terms of the utilization of geothermal resources, so the government targets the installed geothermal capacity to reach four times the previous level by 2025. One important area in the northern part of Sumatra Island is Seulawah Agam, where the Indonesian government has scheduled to build a power plant. Several studies that have been carried out on the volcano are still regional modeling the geothermal system to a depth of 5 km, which includes information on the heat source to reservoir layers using 2D inversion of magnetotelluric and transient electromagnetic data [4], as well as a 3D resistivity model from MT data which shows the overall fault distribution in the volcanic area [6]. The study has shown that the reservoir zone that is the main target for geothermal is below 2 km. In addition, remote sensing studies have also been carried out in the area, including using Landsat Series data [5], and temperature observations using the FLIR sensor [19]. The results of this study indicate an increase in temperature in direct contact with craters and hot springs.

Seulawah Agam is one of the stratovolcano-type volcanos in Aceh Besar Regency, Aceh Province, Indonesia. Tectonically, volcanic activities of Seulawah Agam are controlled by Great Sumatran Fault, spreading across 1900 km from Lampung up to the Andaman Sea [20], [21]. This fault is divided into 20 segments [22], [23], where Seulawah Agam is close to the Seulimum segment, becoming the primary control of the volcano. Besides, results from 3D resistivity also showcase several local faults directly interconnected with manifestations [6], [24], which is ascribed to the primary function of the fault and fracture on the geothermal area of being the main access for fluid transportation from the reservoir layer to the surface [2]. Based on the geological map provided by previous studies [25], [26], the Seulawah volcano is dominated by LamTeuba formation, in which rocks consist of basalt, andesite, tuff, agglomerate, and ash flow. In Seulawah Agam, some surface manifestations are in the South, close to the volcano peak (Ceumpaga crater). Meanwhile, in the Northern part, the manifestation of the Heutsz crater could be found. Both of the preceding craters were relatively big. The activities of the volcano could be attributed to the emergence of several manifestations on the surface; in Ieu Suum, Kreung Raya (located in the northwest), and other manifestations, including Ie Broek and Ie Jue [6], [8].

3 BASIC THEORY AND METHODOLOGY

3.1 VLF-EM

VLF is an electromagnetic method where its source is generated by electromagnetic radiation from a military navigational radio transmitter [15]. This technique operates in the low-frequency range from the 15 – 30 kHz band, which is emitted as the main electromagnetic field transmitted through radio signals as groundwave by the earth's core and ionosphere [13], [27]. The VLF signal detected by the receiving device is a total magnetic field H_R obtained from the primary field H_p and spreads through the air together with the secondary field H_s ; this field is generated from the induction process in the anomaly of the conductor below the surface. The magnitude of the EM field response measured at the receiver will have a different phase between the two secondary and primary fields. Mathematically it can be described as follows:

$$H_R = H_p + H_s H_R = |H_p| e^{i\omega t} + |H_s| e^{i(\omega t - \varphi)} \quad (1)$$

where $H_p \gg H_s$, with the transmitter's frequency (ω) and shifting phase (φ) between the two components of the magnetic field. The parameter could be processed for the determination of a conductivity layer from a conductor located on the subsurface, and the magnetic vector can be shown as eq.2;

$$\begin{pmatrix} 0 \\ H_{RY} \\ H_{RZ} \end{pmatrix} = \begin{pmatrix} 0 \\ H_{PY} \\ 0 \end{pmatrix} + \begin{pmatrix} 0 \\ H_{SY} \\ H_{SZ} \end{pmatrix} \quad (2)$$

Data from the VLF-EM measurement are obtained from in-phase and out-phase ratios of H_{RZ}/H_{RY} reflecting the change of resistivity distribution on the subsurface. Specifically, in-phase data are magnetic field responses against the artificially structural change that has undergone a disturbance due to anthropogenic activities. Meanwhile, out-phase data are electromagnetic field responses against the vertical change on the subsurface. Both parameters of this measurement could be used to investigate the characteristics of shallow subsurface faults [15].

The concept of VLF measurement relies on the assumption of a 2D model of a conductivity layer on the subsurface, where the x-axis corresponds to a geological feature and a pointer to the VLF-EM transmitter. It is used to obtain induced solid anomalies, while the y-axis is the profile measurement for VLF-EM data collection. Therefore, GSM 19 instrument is used to determine the component of vertical (H_z) and horizontal (H_y) from the magnetic field, in which at each data collection point scalar tipper B is obtained from $H_z = B H_y$, as a difference of time between vertical and horizontal magnetic field component during electromagnetic induction phenomenon [2]. This tipper data are the main component required to invert the 2D data of VLF-EM [2]. The difference in polarity between the two primary and secondary magnetic components can result in a difference between the resistive and conductive areas of the subsurface anomaly. Both of these components have similar polarity on the resistive layer, but the phase is different in the conductive anomaly. In general, VLF-EM interpretation could be performed through qualitative and quantitative interpretation. The qualitative approach mainly uses the Fraser or K-Hjelt filter [28] to recognize the lateral resistive

or conductive layers. Meanwhile, a quantitative approach can be made by inverting the data to yield the 2D subsurface resistivity variation.

3.2 Electrical Resistivity

The electrical resistivity relies on the electrical estimation due to the potential gap from the electrode injection. The resistivity method is commonly used to produce the subsurface resistivity variation against the depth using vertical electrical sounding (VES), known as 1D resistivity. The result also can deploy in the profile measurement to obtain information on 2D lateral resistivity variation [26]. Electrode configuration on electrical resistivity works by injecting two current electrodes, such as electrodes at A and B, which are connected to the transmitter source. In comparison, two potential electrodes, M and N, are connected to a voltmeter. The current intensity parameters are arranged in series, and the potential difference ΔV between electrodes M and N are measured [12], [24]. Mathematically, apparent resistivity ρ_A is calculated as follows:

$$\rho_A = K \frac{\Delta V}{I} \quad (3)$$

where K is a geometry factor depending on the electrode array, while $I = MN/2$ and $L = AB/2$.

3.3 Survey Design

To study the shallow hydrothermal of Seulawah volcano manifestations, such as the fault distribution, fracture, fluid direction, and fault geometry that the primary mechanism of manifestation composes, the measurement using VLF-EM and electrical resistivity method across the hot spring le Jue area as shown in Fig. 2. Based on the survey observation, the VLF-EM data were acquired at 4 profiles crossing the hot spring anomaly. After that, the distance between points was made by 10 m to produce the subsurface conductive anomaly with high resolution. Meanwhile, the distance between profiles was also made 100 m with a trajectory length of 700 m to cover the entire area of manifestation le Jue. The electrical resistivity was measured in the same location where the VLF-EM method was carried out with the target depth ranging from 60 – 80 m under the surface using the Wenner-Schlumberger configuration sensitive to the subsurface lateral change [29]. Survey design of VLF-EM and electrical resistivity measurement on manifestation le Jue is shown in Figure 2a, including several documentations of hot spring outcrop – by Figure 2b and measurement of on-ground VLF-EM observation using GEM equipment – Figure 2c.

In this research, the VLF-EM data was acquired using GEM Systems GSM 19-T equipment which was operatable with two frequencies simultaneously. Based on the geographical location and the alignment of frequency choice, we employed frequency 19.8 kHz (NWC) transmitted from Exmouth and Western Australia and 21.4 kHz (NPW) from Hawaii because both frequencies are good in quality, where the tolerance limit obtained reached 12%. Furthermore, most VLF transmitters operate for 24 h. Still, several other VLF-EM transmitters were shut down for maintenance purposes with pre-determined schedules, so the data collection should be adjusted with the preceding schedules in each station of the VLF-EM transmitter.

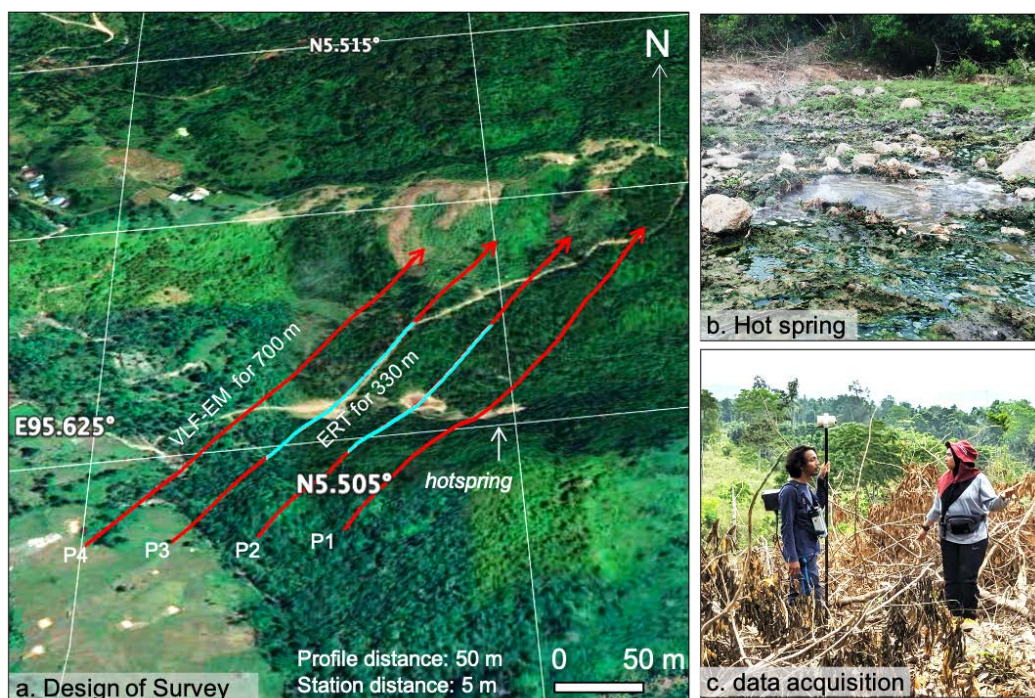


Fig.2 (a). Description of VLF-EM and electrical resistivity data collection on the area of hot spring le Jue, Seulawah Agam volcano. The measurement profile of VLF-EM is shown by red and resistivity–green color. (b) hot spring outcrop captured from the investigated area with temperatures > 100°C. (c) documentation of VLF measurement using GSM-19 equipment.

4 RESULTS AND INTERPRETATION

4.1 Current Density and Fraser

Based on the observational data, parameters obtained from GSM-19 are in-phase and out-phase values as the ratio between the vertical and horizontal magnetic field in the same phase but in a different phase with a primary field. Both parameters were pre-processed with the average moving technique to eliminate the noise or effects from the near-surface field. The transmitter's distance being far away from the measuring site contributed to a more challenging interpretation of the subsurface anomaly. Furthermore, filtered data were analyzed qualitatively using Fraser and current density, which could represent the subsurface anomaly. Referring to the previous research, the Fraser filter could convert the intersection of in-phase or out-phase data, capable of indicating the anomaly position of conductive material on the subsurface, where the center of the conductive material was suspected to be located right under the peak of Fraser-filtered data [2], [30]. The anomaly of VLF-EM data could be identified from the intersection between in-phase and out-phase curves. The conductive anomaly was marked by the positive value of the in-phase curve and the negative value of the out-phase curve.

In contrast, the resistive anomaly is indicated by the negative value of the in-phase curve and the positive value of the out-phase curve. The fundamental principles of the Fraser filter are using VLF-EM data from four sequential stations by subtracting the sum of the third and fourth data against the first and second data. The following equation could calculate the mathematical expression of the Fraser value:

$$F_{2,3} = (H_3 + H_4) - (H_1 + H_2) \quad (4)$$

The results were acquired from points H_2 and H_3 from in-phase or out-phase stations. Moreover, we also applied the Karous-Hjelt filter to produce the electrical current density variation on earth against depth [30]. The equivalent current density was obtained from the filtered in-phase components at a constant depth in the resulting magnetic field. Karous-Hjelt is a filter developed based on the Biot-Savart law to explain the vertical part of the magnetic field correlated with electrical current. This filter generates the depth trajectory of the electrical current density derived from the vertical component of the magnetic field at each measuring point. Current density is a parameter that is proportional to subsurface electrical conductivity, where the mathematical expression is shown as follows:

$$\left(\frac{\Delta z}{2\pi}\right) I_a \left(\frac{\Delta x}{2}\right) = -0.205 H_{-2} + 0.323 H_{-1} - 1.446 H_0 + 1446 H_1 - 0.323 H_2 + 0.205 H_3 I_a(x/2) \quad (5)$$

where Δz is the assumption of the thickness of a layer for the cross-sectional area of charge density, with Δx as the distance between the measuring points and is assigned as a depth of a layer, while H_{-2} to H_3 is the normalized value of the vertical magnetic field (H_z/H_y) at six measuring points. Figure 3 shows the Fraser analysis and current density at 4 VLF-EM measuring locations in le Jue. The Karous Hjelt filter is applied to facilitate the interpretation of anomalies below the surface. The current density parameter of this filter is related to the electrical properties of rocks concerning depth, such as conductivity. The 2D model of this technique can be mapped by a subsurface structure model based on the electrical properties of the material, which is very sensitive to the electromagnetic method [31], the density model of VLF-EM is shown in Figure 3.

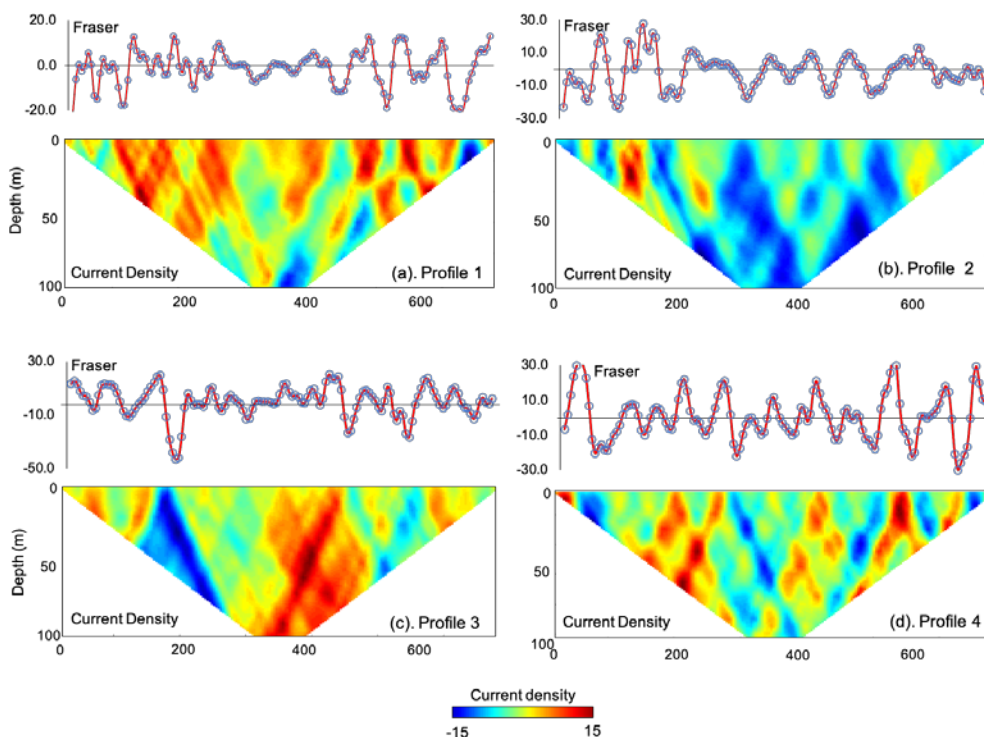


Fig.3. Qualitative analysis of Fraser and current density applied on the four VLF-EM profiles. The values obtained from current density and Fraser analysis are directly proportionate toward electrical conductivity.

In profile 1 (Fig.3a) the Fraser values were varied within the range of -20 to 20%, where theoretically, the high Fraser amplitude could be considered a conductive zone, while the low values represent the resistive layer on the subsurface. Besides, if the amplitude is small, the value could represent a shallow anomaly source, and the high wavelength is a response from a deep anomaly source. In profile 1, the Fraser value is relatively high in several locations, suspected as a response to the conductive anomaly, which could also be observed on current density data that are commonly high. This anomaly is also suspected to respond to the presence of volcanic manifestations such as warm ground and hot springs. Moreover, in several other locations, such as those at 0—10 m, 280—320, and 650—799 m, the resistive anomaly, suspected as rock components of Seulawah Agam volcano, are shown in low Fraser value and low current density.

Profile 2 (Figure 3b) has a more resistive anomaly than profile 1, but the conductive anomaly represents several points. For example, at a distance of 80-150 m, the Fraser value and current density were high (10—30%) suspected as a response to the presence of subsurface manifestation, which was similarly observed at a 200—250 m distance as a response for the warm ground layer of Seulawah Agam manifestation. The high value of the current density anomaly is located at 30-m deep under the surface. However, the depth obtained from this filter is a numerical calculation based on the extended analysis of the measuring profile. On the centre of the profile, the low current density is suspected to be the basic rock of the measuring area, which is relatively resistive compared with volcanic manifestations. The third profile (Figure 3c), was based on the observational data manifestation at a 250—300 m distance and had a relatively high Fraser value of up to 30%.

Compared with other areas, this anomaly is characterized by high current density values at a depth of 50 m. It is suspected of responding to a fault or fracture, which is usually conductively associated with the fluids filling the rocks. The previous studies explained that the fault in geothermal systems functions as access media of the fluid from the reservoir layer into the surface layer, allowing the presence of manifestation strongly correlated with fault activities or subsurface fracture [2], [9]. On the other side of profile 3, several conductive zones were obtained with smaller geometry at shallow depth, for instance, at 200—250 and 500—530 m, which could be presumably associated with surface manifestations such as warm ground and hot springs. In profile 4 (Figure 3d), the distribution of Fraser value and current density is observed to variation. For example, at a 200—250 m distance, the values were obtained high as the representative of conductive anomaly, where the generated pattern of this anomaly is a vertical dyke up to 50 m depth under the surface, where the same anomaly was also observed at 400—450 and 600—640 m distances from the measuring profile which could be suspected as a response from subsurface fracture and minor fault activities. In general, anomaly patterns generated for profiles 1, 3, and 4 were similar to fracture or fault anomalies with conductive properties. Nonetheless, there is a difference in profile 2, which is generally resistive but with the same pattern. Considering the Karous filter is a qualitative interpretation, so for further interpretation we validated the VLF-EM data with electrical resistivity (which is often applied for a near-ground survey).

4.2 Comparison to Electrical resistivity

Following the current density model from the four VLF-EM routes, validation was required from the resistivity model provided by previous research [32] employing 180 – 510 m distance measurement from profiles 2 and 3 of VLF-EM. Thus, the depth of the resistivity model obtained was 320 m. The VLF-EM model was only plotted in the same location as the electrical resistivity to ease the interpretation. Referring to published literature, a combination between VLF-EM and electrical resistivity should yield accurate results for delineating subsurface structure because both methods possess good sensitivity against electrical conductivity [18]. Moreover, we plotted VLF-EM data with the electrical resistivity using different scale colours because the resistivity parameter is disproportional toward conductivity or current density from VLF-EM, as shown in Figure 4.

Based on profile 2, VLF-EM and electrical resistivity data could exhibit the same model, especially at 150—200 m, where a low resistive anomaly characterizes the area in response to a high conductive zone. The anomaly was suspected of fault and fracture crossing the subsurface layer as the exit route of geothermal fluids to the surface. This fault becomes the primary mechanism of shallow hydrothermal construction from le Jue manifestation, Seulawah Agam. This anomaly structure could be clearly seen in the electrical resistivity model characterized by resistivity structure dipping down up to 40 m depth. VLF-EM mode also shows the anomaly through high current density patterns at a relatively similar depth.

Profile 3, also measured around profile 2, showed better responses obtained from the electrical resistivity and VLF-EM. At 100—180 m, it was demonstrated by a conductive zone characterized by high current density and low resistivity. Meanwhile, at 200—300 m, the response was a resistive anomaly. Both methods could clearly show both zones, where the presence of suspected faults or fractures was depicted at 180—200 m from the measuring profile. This anomaly has a vertical property with a depth of up to 40 m under the surface. Nonetheless, on the Westside, where the resistivity data showed a conductive anomaly, VLF-EM data could not depict the anomaly contrast owing to the response from horizontal hot springs or warm ground anomaly. VLF-EM and electrical resistivity models are generally similar, whereas the conductivity model could be very well mapped. This indicates that the data quality and effectiveness of the VLF-EM method can be used for subsurface interpretation. On the other side, VLF current density model could merely depict vertical anomaly structures such as dike or fracture. In contrast, horizontal anomalies such as near-surface conductive hot springs and warm ground anomalies could be well represented in the electrical resistivity model. These findings are understandable since the current density model is a qualitative analysis,

requiring further process using the Occam model for 2D inversion against VLF-EM data. This way true resistivity and depth parameters could be obtained as in the electrical resistivity method.

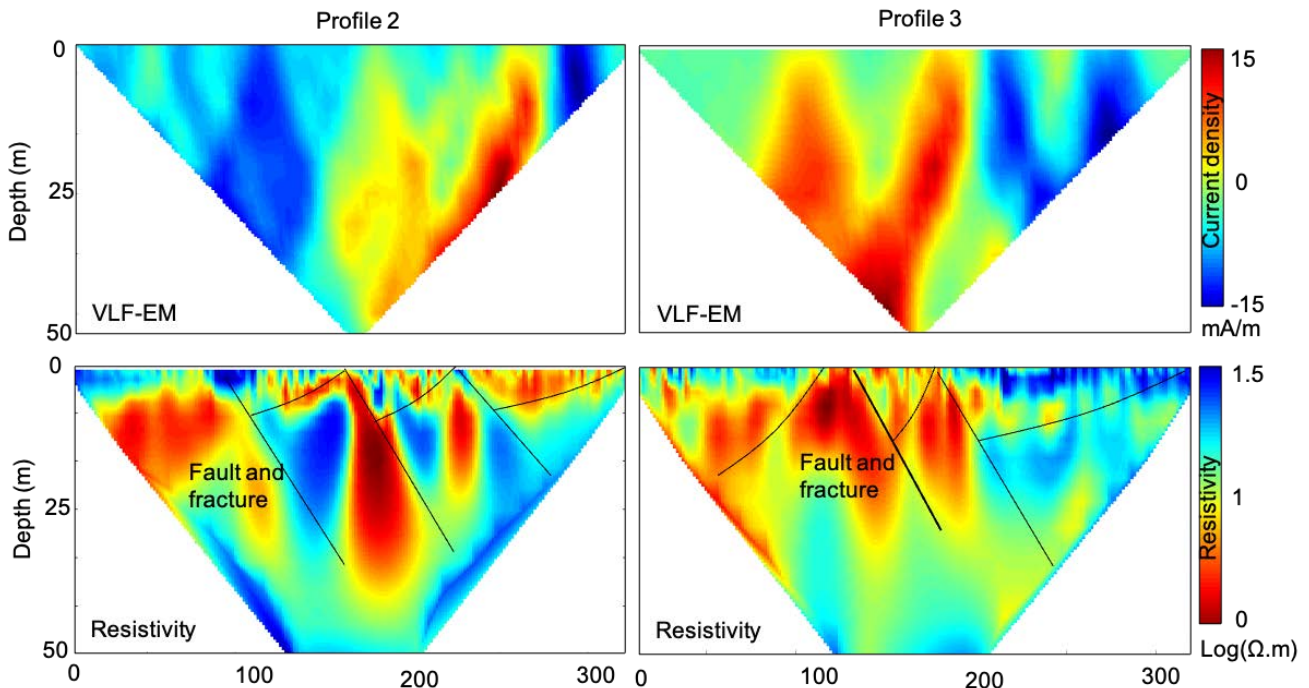


Fig.4. Comparison between electrical resistivity data with VLF-EM current density. The resistivity profile was measured at 300 m from profiles 2 and 3 of VLF-EM, as shown in the survey design. Current density data is disproportional against resistivity, allowing both data to be plotted on opposite scales bare.

4.3 2D Inversion of VLF-EM

The inversion process is carried out to interpret the quantitative data of VLF-EM against the depth function. Inversion could be defined as the processing of observed data involving mathematical solving techniques to acquire subsurface distribution physical properties of the subsurface. Similarly to electromagnetic methods, VLF-EM could be inverted to obtain the true resistivity value based on transmitter frequency and ambient resistivity [30], [33]. Inv2DVLF software has been developed by [34] to quantitatively interpret the single frequency by employing a regulated 2D inversion approach. The resistivity model obtained had RMS error varied from 2.5 – 20.3 %, as shown in Fig.5. The reasonable and representative initial resistivity for the entire surrounding condition is equal to 100 Ω used as the initial parameter when VLF inversion was carried. In profile 1 (Figure 5a), the resistivity value displayed in the logarithmic scale varied from 2 to 75 m depth under the surface. The 2D model showed the conductive and resistive area distribution up to 35 m depth, while further depth was lateral. The conductive anomaly with a resistivity value of $<1 \Omega\text{m}$ is strongly associated with volcanic activities. This could also be observed in profile 2 (Figure 5b) at a distance of 200–700 m, where the conductive anomaly was elongated at a depth < 20 m. this anomaly was suspected as a response against the surface manifestation such as Hotspring, fumaroles, and warm ground. The inversion results of both profiles are reliable since the RMS values were small; 5.5% and 2.5% for profiles 1 and 2, respectively.

Meanwhile, in profile 3 (Figure 5c), the resistivity distribution was obtained relatively differently on the Westside, but the same response was received on the Westside, where conductive anomaly indicates the volcanic activities. Similarly, in profile 4 (Figure 5d), the resistivity patterns relatively correspond with that in profile 3. Based on the high RMS obtained on profiles 3 and 4 (25.7% and 20.3%, respectively), both profiles could not be used for further interpretation because of bad accuracy. Nonetheless, apart from the fact that the Westside was relatively similar to other profiles, the West side of profile 3 was observed with a conductive zone at 35–50 m under the surface, which was strongly associated with the volcano, where it could be well traced on resistivity models of profile 1 and profile 2 with small RMS values.

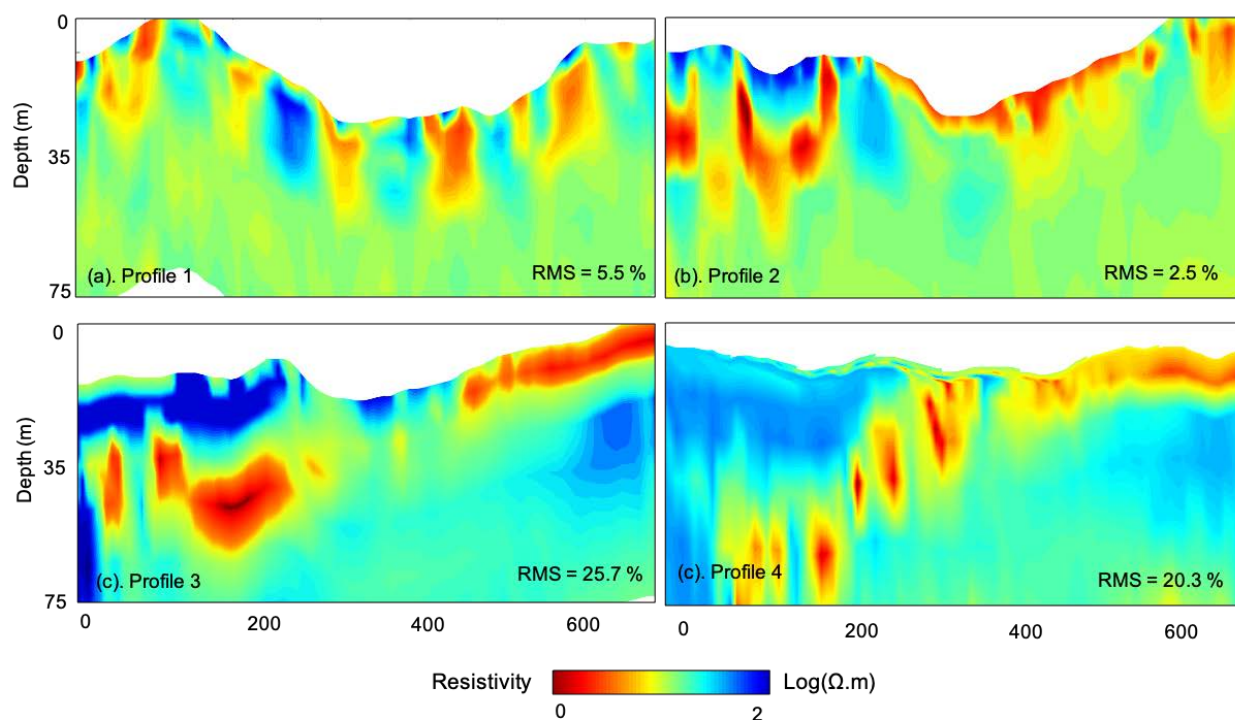


Fig.5. Inversion of 2D data VLF-EM with single frequency using Occam algorithm and overlaid with topography from Google Earth. (a) profile 1 with RMS=5.5%, (b) Profile 2 with the lowest RMS of 2.5%, meanwhile for profile 3 (c) and profile 4 (d) the relatively high RMS values were obtained, they were 25.7% and 20.3%, respectively.

5 DISCUSSION

Referring to a previous report [35], there are several reservoir systems types geothermal which could be used to produce electrical energy, yet hydrothermal is the most commonly used, including in Indonesia, where the system contains gaseous or liquid fluid (or its combination) depending on the subsurface reservoir pressure and temperature. The hydrothermal technique in a volcano area is regulated by the fault and fracture activities acting as the exit and entrance of the fluid. Therefore, it is important to study local geological structures in geothermal energy power plants because different local geologies govern each volcanic manifestation. The magneto-telluric and micro-seismic applications could be used to investigate deep geothermal anomalies [6], [36], while resistivity and VLF methods are more dominant to be applied for shallow anomalies [2], [37]. Figure 6 is a hydrothermal system from Ie Jue manifestation showing the distribution of faults and fractures based on the VLF-EM resistivity data.

VLF-EM inversion has provided a picture of the subsurface and shallow hydrothermal conditions of Ie Jue manifestations. On the Westside, at 180–200 m distance, a conductive anomaly with resistivity below $1 \Omega\text{m}$ was observed at 30 m depth. The anomaly was suspected as the area for the fluids gathered from reservoirs. The fluids then surge to the surface, between 150 and 200 m distances, resulting in fumarole and warm ground manifestations. This surging process through fractures and faults becomes the regulator of the manifestation, as observed on the black lines in Figure 6.

Furthermore, anomalies with high resistivity were obtained on the near-surface area, where the area was suspected of as-deposited materials of resistive hard rock. At a 300–600 m distance with 30 m depth, the conductive layer was found elongated near the surface, where the anomaly was suspected as a response from fumarole and warm ground manifestations, corroborated by the on-ground observation showing the presence of hot spring with temperatures $>100^\circ\text{C}$. The constructed 2D model also shows several conductivity zones filled with resistive parts represented by fractures or local faults. This could also be seen on the West side of the measuring profile (600–700 m), where conductive zones as 30 depth could be interpreted as warm ground area. The fault distribution could be mapped very well on the 2D VLF-EM model. Even the fault straightness to 50 m depth giving information about the fluid access from the clay cap layer to the surface could also be very well depicted. Therefore, the same technique could be used to investigate shallow hydrothermal structures in other volcanic areas, especially in Indonesia famous for its tropical forests and high terrain. In reality, the application of VLF has been very well utilized to investigate groundwater [34], archaeology [27], and near-fault structures [38].

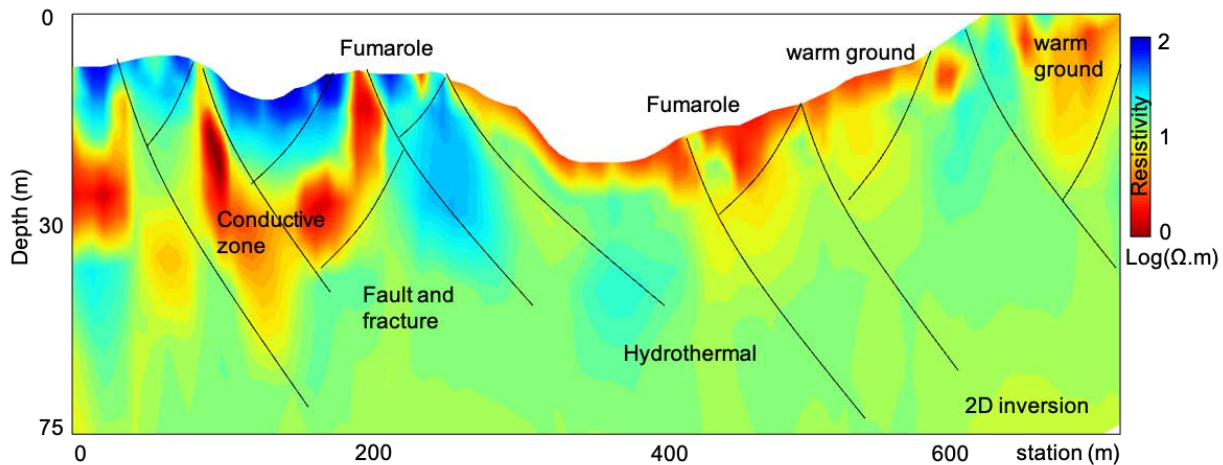


Fig. 6. Resistivity data against the depth acquired from 2D inversion of VLF-EM data, where the 2D model was overlaid with the outcrops manifestation and fault estimation from on-ground observation.

However, the utilization is still relatively scarce for geothermal studies, especially in Asia. Two advantages of VLF-EM include its efficiency and easy on-ground mobility as compared with other near-surface methods such as electrical resistivity, GPR, or seismic at high terrain conditions [2], [37], [39]. Differently with the state of volcanos in Europe and others located in low terrain areas, the instrument's mobility was not considered as much. Therefore, developing the VLF method for geothermal can be applied to locations with high terrain conditions. Yet, the model should be validated with other geophysical approaches to yield a comprehensive result.

6 CONCLUSIONS

Studies on geothermal energy are often associated with using the conventional magnetotelluric method in mapping the geothermal system in deep areas such as heat sources, reservoirs, and clay caps. However, constructing a powerplant requires injection and production wells, demanding studies on local faults of each manifestation to avoid the drilling error that could result in a great industrial cost. In general, for shallow exploration, the resistivity method is highly potential. Nonetheless, the technique is not considered effective for volcanos with high terrain and remote areas due to complex mobility requiring many field personnel. Herein, we have surveyed VLF-EM data on 4 profiles with a length of 700 m in each profile. This exploration was performed to predict the geometry of the fault and fracture structures associated with the shallow hydrothermal system from Ie Jue manifestation. The qualitative analysis results through several filters generate high values suggesting the interconnection of several faults or fractures that are mostly dyke or vertical. This conductive anomaly is observed through a Fraser value of $> 20\%$ and a current density of > 5 . On the other side, the anomaly contrast is also shown on the electrical resistivity data as a conventional near-surface structure measured on the same site of VLF-EM.

We also applied the Occam algorithm to quantitatively analyzed VLF-EM data in the form of 2D inversion resulting in resistivity data as a standard parameter in the electromagnetic method. The results of the 2D modeling could depict very well the hydrothermal system, where the presence of fault and fracture becomes the access media for fluid to surge to the surface. This could be traced very well through the low resistivity parameter (log resistivity of $0-1 \Omega\text{m}$). Apart from faults, this cross-section model also shows the presence of conductive anomaly on the area near the surface, suspected as a response to the presence of fumarole and warm ground manifestations. Based on the 2D inversion model, it can be concluded that the VLF-EM method for shallow hydrothermal investigation is highly potential to be developed, especially since this model could be mobilized by just one person, resulting in efficiency when applied to other volcanos that have high terrain condition such as those in tropical countries.

7 ACKNOWLEDGMENT

The authors acknowledge and appreciate the contributions of the Geophysical Engineering students for assisting the acquisition of VLF-EM and electrical resistivity data in Ie Jue. The research is fully funded by Calon Professor 2022 research grant from Universitas Syiah Kuala with a No: 068/UN I1.2.1/PT.01.03/PNBP/2022. The authors also thanks to Fernando A Monteiro Santos for providing the codes of PrepVLF and Inv2DVLF.

8 REFERENCES

- [1] Hochstein, M. P., Sudarman, S. (2008). History of geothermal exploration in Indonesia from 1970 to 2000. *Geothermics*, vol. 37, no. 3, 220–266, DOI: 10.1016/j.geothermics.2008.01.001
- [2] Yanis, M., Ismail, N., Abdullah, F.(2022). Shallow Structure Fault and Fracture Mapping in Jaboi Volcano, Indonesia, Using VLF–EM and Electrical Resistivity Methods. *Natural Resources Research*, vol. 31, no. 1, 335– 352, DOI: 10.1007/s11053-021-09966-7.

- [3] Yanis, M., Novari, I., Zaini, N., Marwan., Pembonan, A.Y., Nizamuddin. (2020). OLI and TIRS Sensor Platforms for Detection the Geothermal Prospecting in Peut Sagoe Volcano, Aceh Province, Indonesia. International Conference on Electrical Engineering and Informatics (ICELTICs), p. 1-6.
- [4] Marwan., Yanis, M., Idroes, R., Ismail. (2019). 2D inversion and static shift of MT and TEM data for imaging the geothermal resources of Seulawah Agam Volcano, Indonesia. International Journal of GEOMATE, vol. 17, no. 62, 173-180, DOI: 10.21660/2019.62.11724.
- [5] Zaini, N., Yanis, m., Marwan., Isa, M., Van Der Meer, F. (2021). Assessing Of Land Surface Temperature At The Seulawah Agam Volcano Area Using The Landsat Series Imagery. Journal of Physics: Conference Series, P.0122021.
- [6] Marwan., Yanis, M., Nugraha, G.S., Zainal, M., Arahman, N., Idroes, R., Dharma, D.B., Saputra, D., Gunawan, P. (2021). Mapping of Fault and Hydrothermal System beneath the Seulawah Volcano Inferred from a Magnetotellurics Structure. Energies, vol. 14, no. 19, 6091, DOI: 10.3390/en14196091.
- [7] Marwan., Yanis, M., Zainal, M., Nugraha, G.S. (2020). Application Of QR Codes As A New Communication Technology And Interactive Tourist Guide In Jaboi, Sabang. IOP Conference Series: Materials Science and Engineering, p. 012025.
- [8] Idroes, R., Yusuf, M., Saiful., Alatas, M., Subhan., Lala, A., Muslem., Suhendra, R., Idroes, G.M., Marwan., Mahlia, T.M.I. (2019). Geochemistry Exploration and Geothermometry Application in the North Zone of Seulawah Agam, Aceh Besar District, Indonesia. Energies, vol. 12, no. 23, 4442, DOI: 10.3390/en12234442.
- [9] Zhang, L., Jiang, P., Wang, Z., Xu, R. (2017). Convective heat transfer of supercritical CO₂ in a rock fracture for enhanced geothermal systems. Applied Thermal Engineering, vol. 115, 923–936, DOI: 10.1016/j.applthermaleng.2017.01.013.
- [10] Ebrahimi, A., Sundararajan, N., Babu, V.R. (2019). A Comparative Study For The Source Depth Estimation Of Very Low Frequency Electromagnetic (VLF-EM) Signals. Journal of Applied Geophysics, vol.162, 174-183, DOI: 10.1016/j.jappgeo.2019.01.007.
- [11] Drahor, M. G., Berge, M. A. (2006). Geophysical investigations of the Seferihisar geothermal area, Western Anatolia, Turkey. Geothermics, vol. 35, no. 3,302–320, DOI: 10.1016/j.geothermics.2006.04.001.
- [12] Özürlan, G., Sahin, M.H. (2006). Integrated Geophysical Investigations In The Hisar Geothermal Field, Demirci, Western Turkey. Geothermics, vol. 35, no. 2, 110–122, DOI: 10.1016/J.GEOTHERMICS.2005.11.004.
- [13] Lin, M.J., Jeng, Y. (2010). Application Of The VLF-EM Method With EEMD To The Study Of A Mud Volcano In Southern Taiwan. Geomorphology, vol. 119, no. 1–2, 97–110, DOI : 10.1016/J.GEOMORPH.2010.02.021.
- [14] Niculescu, B.M., Andrei, G. (2019). Using Vertical Electrical Soundings To Characterize Seawater Intrusions In The Southern Area Of Romanian Black Sea Coastline. Acta Geophysica, vol. 67, no. 6, 1845–1863, DOI: 10.1007/s11600-019-00341-y.
- [15] Chabaane, A., Redhaounia, B., Gabtni, H. (2017). Combined Application of Vertical Electrical Sounding And 2D Electrical Resistivity Imaging For Geothermal Groundwater Characterization: Hammam Sayala Hot Spring Case Study (NW Tunisia). Journal of African Earth Sciences, vol. 134, 292–298, DOI: 10.1016/j.jafrearsci.2017.07.003.
- [16] Marwan., Idroes,R., Yanis, M., Idroes, G.M., Syahriza. (2021). A Low-Cost UAV Based Application For Identify and Mapping a Geothermal Feature in Ie Jue Manifestation, Seulawah Volcano, Indonesia. International Journal of GEOMATE, vol. 20, no. 80, 135–142, DOI: 10.21660/2021.80.j2044.
- [17] Yanis, M., Abdullah, F., Zaini, N., Ismail, N. (2021). The Northernmost Part Of The Great Sumatran Fault Map And Images Derived From Gravity Anomaly. Acta Geophysica, vol. 69, no. 3, 795–807, DOI: 10.1007/s11600-021-00567-9.
- [18] Yanis, M., Abdullah, F., Yenny A., Zainal, M., Abubakar M., Ismail, N. (2020). Continuity of Great Sumatran Fault in the Marine Area revealed by 3D Inversion of Gravity Data. Jurnal Teknologi, vol. 83, no. 1, 145–155, DOI: 10.11113/jurnalteknologi.v83.14824.
- [19] Sieh, K., Natawidjaja, D. (2000). Neotectonics Of The Sumatran Fault, Indonesia. Journal of Geophysical Research: Solid Earth, vol. 105, no. B12, 28295–28326, DOI : 10.1029/2000JB900120.
- [20] Rizal, M., Ismail, N., Yanis, M., Zainal, M., Surbakti, M.S. The 2d Resistivity Modelling On North Sumatran Fault Structure By Using Magnetotelluric Data. Iop Conference Series: Earth And Environmental Science, p. 012036.
- [21] Ismail, N., Yanis, M., Idris, S., Abdullah, F., Hanafiah, B. (2017). Near-Surface Fault Structures of the Seulimuem Segment Based on Electrical Resistivity Model. Journal of Physics: Conference Series, p. 012016.
- [22] Bennett, M.R., Doyle P. (Geology On Your Doorstep). Geology Society, p. 270.
- [23] Yanis, M., Marwan., Paembonan, A.Y., Yudhyantoro, Y., Rusydy., Idris, S., Asrillah. (2022). Geophysical and Geotechnical Approaches in Developing Subsurface Model for Gas Power Plant Foundation. Indian Geotechnical Journal, vol.52, 237-247, DOI: 10.1007/s40098-021-00559-y.

- [24] Yanis, M., Bakar, M.A., Ismail, N. (2017). The Use of VLF-EM and Electromagnetic Induction Methods for Mapping the Ancient Fort of Kuta Lubok as Tsunami Heritage i. 23rd European Meeting of Environmental and Engineering Geophysics, p. 1-5.
- [25] Karous, M., Hjelt, S.E. (1983). Linear Filtering of VLF Dip-Angle Measurements. Geophysical Prospecting, vol. 31, no. 5, 782–794, DOI: 10.1111/j.1365-2478.1983.tb01085.x.
- [26] Yanis, M., Zainal, M., Marwan, Ismail, N. (2019). Delineation of Buried Paleochannel Using EM Induction in Eastern Banda Aceh, Indonesia. 81st EAGE Conference and Exhibition 2019, p. 1-5.
- [27] Majumdar, R.K. Majumdar, N., Mukherjee, A.L. (2000). Geoelectric investigations in Bakreswar geothermal area, West Bengal, India. Journal of Applied Geophysics, vol. 45, 187-202, DOI : 10.1016/S0926-9851(00)00028-8.
- [28] Sungkono., Husein, A., Prasetyo, H., Bahri, A.S., Santos, F.A.M., Santosa, B.J. (2014). The VLF-EM Imaging Of Potential Collapse On The LUSI Embankment. Journal of Applied Geophysics, vol. 109, 218–232, DOI: 10.1016/j.jappgeo.2014.08.004.
- [29] Idris, S., Syukri, M., Surbakti, M.S., Marwan., Muchlis., Rusydy, I., Aflah, N. (2018). Analysis Of Shallow Subsurface Structure At Geothermal Area Of Ie Jue Using Resistivity Method. Jurnal Natural, vol. 18, no.1, 18-21, DOI: 10.24815/JN.V18I1.9676.
- [30] Ismail, N., Nadra, U., Yanis, M. (2021). Understanding Volcano Activity Using 2D Simulation Models of MT Data. The 2nd SEA-STEM International Conference, p. 129–132.
- [31] Santos, F.A.M, Mateus, A., Figureas, J., Golcanves, M.A. (2006). Mapping Groundwater Contamination Around A Landfill Facility Using The Vlf-Em Method - A Case Study. Journal of Applied Geophysics, vol. 60, no.2, 115-125, DOI: 10.1016/j.jappgeo.2006.01.002
- [32] Nasruddin, M., Alhamid, I.Y., Surachman, A.A., Sugiyono, Aditya, H.B., Mahlia, T.M.I. (2016). Potential of geothermal energy for electricity generation in Indonesia: A review. Renewable and Sustainable Energy Reviews, p. 733-740.
- [33] Singarimbun, A., Gaffar, E.Z., Tofani, P. (2017). Modeling Of Reservoir Structure By Using Magnetotelluric Method In The Area Of Mt. Argopuro, East Java, Indonesia. Journal of Engineering and Technological Sciences, vol. 49, no. 6, 833–847, DOI: 10.5614/j.eng.technol.sci.2017.49.6.9.
- [34] Vargemezis, G., 3D Geoelectrical Model Of Geothermal Spring Mechanism Derived From VLF Measurements: A Case Study From Aggistro (Northern Greece). 2014. Geothermics, vol. 51, 1–8, DOI: 10.1016/j.geothermics.2013.09.001.
- [35] Sharma, S.P., Baranwal, V.C. (2005). Baranwal, "Delineation Of Groundwater-Bearing Fracture Zones In A Hard Rock Area Integrating Very Low Frequency Electromagnetic And Resistivity Data. Journal of Applied Geophysics, vol. 57, no.2, 155-156, DOI: 10.1016/j.jappgeo.2004.10.003.
- [36] Marwan, Asrillah, Yanis, M., Furumoto, Y. (2019). Lithological Identification Of Devastated Area By Pidie Jaya Earthquake Through Poisson's Ratio Analysis. International Journal of GEOMATE, vol. 17, no. 63, 210–216, DOI: 10.21660/2019.63.77489.

Paper submitted: 22.05.2022.

Paper accepted: 10.10.2022.

This is an open access article distributed under the CC BY 4.0 terms and conditions